



Secondary mineralogy of Jezero delta rocks from hydrogen and carbon emission lines in supercam libs data

P. Beck, O. Forni, E. Dehouck, O. Beyssac, K. Benzerara, C. Quantin-Nataf, S. Schröder, P.-Y. Meslin, E. Clavé, A. Cousin, et al.

► To cite this version:

P. Beck, O. Forni, E. Dehouck, O. Beyssac, K. Benzerara, et al.. Secondary mineralogy of Jezero delta rocks from hydrogen and carbon emission lines in supercam libs data. 54th Lunar and Planetary Science Conference 2023, Lunar and Planetary Institute, Mar 2023, The Woodlands, Texas, United States. pp.1241. hal-04034961

HAL Id: hal-04034961

<https://hal.science/hal-04034961>

Submitted on 17 Mar 2023

HAL is a multi-disciplinary open access archive for the deposit and dissemination of scientific research documents, whether they are published or not. The documents may come from teaching and research institutions in France or abroad, or from public or private research centers.

L'archive ouverte pluridisciplinaire **HAL**, est destinée au dépôt et à la diffusion de documents scientifiques de niveau recherche, publiés ou non, émanant des établissements d'enseignement et de recherche français ou étrangers, des laboratoires publics ou privés.

SECONDARY MINERALOGY OF JEZERO DELTA ROCKS FROM HYDROGEN AND CARBON EMISSION LINES IN SUPERCAM LIBS DATA. P. Beck¹, O. Forni², E. Dehouck³, O. Beyssac⁴, K. Benzerara⁴, C. Quantin-Nataf⁵, S. Schröder⁶, P.-Y. Meslin², E. Clavé⁷, A. Cousin², P. Pilleri², J. Lasue², W. Rapin², R.B. Anderson⁸, O. Gasnault², T.S.J. Gabriel⁸, A.J. Brown⁹, S. Maurice², R.C. Wiens¹⁰ ¹IPAG, Grenoble France (pierre.beck@univ-grenoble-alpes.fr), ²IRAP, Toulouse, France, ³LPG, Nantes, France, ⁴IMPMC, Paris, France, ⁵LGL-TPE, Lyon, France, ⁶DLR-OS Berlin, Germany, ⁷LAB, Bordeaux, France, ⁸USGS, Flagstaff, USA, ⁹Plancius Research, MD, ¹⁰Purdue University, USA.

Introduction: The geomorphologic identification of a delta within the Jezero crater was key in its selection as the M2020 landing site. After slightly more than a year of dedicated investigations of the crater floor [1,2] the Perseverance rover is now providing the first look at rocks and soils from a Martian delta.

Onboard Perseverance, SuperCam is a versatile instrument, that offers a multi-technique-based remote analysis of chemistry and mineralogy in the rover's proximity [3,4]. This instrument can probe primary and secondary mineralogies with vibrational spectroscopy (infrared [IR] and Raman), as well as chemistry using laser-induced breakdown spectroscopy (LIBS).

The LIBS technique can determine major element abundances, as well as abundances of certain minor elements. SuperCam is unique among other instrument onboard Perseverance due to its ability to directly detect light elements (H, Li, C, N) using its LIBS mode. Here we focus on carbon and hydrogen in rocks from the delta following our earlier work on the crater floor presented last year [5].

Methods: While in [5] we used hydrogen ICA score, in this work we performed a spectral fitting of the region around 650-660 nm where the hydrogen signal occurs. The H line at 656 nm is partially overlapping with a carbon doublet (around 658 nm). This spectral region was fitted by two Lorentzian lines corresponding to H and C (the C doublet is not resolved at SuperCam spectral resolution), and two lines at 655 and 659 nm corresponding to iron. The H and C signal is normalized by dividing by the O777 line intensity following earlier work [6-7]. The H and C signals were analyzed for each of the individual laser shots (generally 30) and combined to the LIBS-derived Mean-Oxide-Composition [8]. The first five shots of the laser burst were excluded for this analysis to remove the contribution of eolian dust. We also excluded soils from this analysis since significant eolian transport might occur inside the crater. A distance correction was applied to the carbon signal. We also used the LIBS-infrared fusion approach described in [9], in which IR spectral parameters (slope, band depths) of collocated LIBS and IR analysis are plotted in ternary diagrams.

Results and discussion: In Figure 1 we present the SuperCam data obtained on Jezero delta rocks in ternary

diagrams. These diagrams were designed following the approach presented in [10] for the study of clay minerals and weathering.

Overall hydrogen abundance in delta rocks: In Fig. 1b the ternary diagram is color-coded according to the H656/0777 ratio, and diagrams are shown for rocks from the delta and compared to earlier observation in the Seitah area (Fig1. C,F). These diagrams reveal that, overall, rocks from the delta have a stronger hydrogen signal. Also, it appears that low-hydrogen points attributed to anhydrous silicates (olivine, opx, cpx, feldspar) are much less abundant in delta-rock than in Seitah. We can observe also in this plot that large (>0.35 mm) feldspar grains are absent as pure phase in delta rocks, but on the other hand many analyses made on Delta rocks show elevated Al₂O₃ (>5 wt.%; Fig 1A).

Rock coatings: In both rocks from the Delta and Seitah, we observe the same cluster of points with elevated hydrogen signal. These points are interpreted as indurated dust coatings [5,11]. While the Seitah and Delta protoliths have different chemistry, the identical composition of this cluster confirms its nature as a coating, rather than an alteration rind, and its formation is probably a recent process.

Carbonates: The analysis of the C658/0777 line ratio reveal that most of the Si-poor and Fe- and Mg-rich points from the delta are enriched in carbon (Fig. 1B). This strongly suggests that many of these points correspond to FeMg carbonate. Their Mg# is around 70 and is similar to Mg# of the olivine grains analyzed by SuperCam in the Delta (see also [12-13]).

Phyllosilicates and sulfates: Many of the points analyzed by SuperCam in the lower delta / delta front are enriched in hydrogen compared to anhydrous silicates. This is in agreement with the observation of strong clay mineral signatures in SuperCam VISIR analysis, with metal-OH absorptions around 2.30 or 2.33 μ m [13]. Ca-sulfates were detected by SuperCam in veins but are found to be poor in hydrogen in agreement with the identification of anhydrite using Raman spectroscopy [14]. By combining LIBS and VISIR data, we located in the ternary diagrams the position of the targets showing strong 2.30 and 2.33 μ m infrared signature (Fig 1C). The analysis showing strong 2.33 μ m are mostly from the lower part of delta-

sequence and corresponds to analysis with a rather low Al, high (Mg+Fe)/Si and slightly elevated Ca/Na/K. While the presence of a strong VISIR absorption at 2.33 μm suggests serpentine, LIBS derived chemistry can be reconciled with VISIR only if serpentine is mixed with some amount of a Ca/Na/K-bearing but Al-poor phase. In Fig.1 we also show the location of some points that show a signature around 2.30 μm (Fig. 1C). These points are enriched in aluminum, have an elevated hydrogen signal, and a stoichiometry close but not identical to nontronite. The possible mineralogy corresponding to these points is being investigated.

Acknowledgments: This work has benefited from support from INSU-CNES.

References: [1] Farley K.A. et al., *Science* 377, 6614 (2022) [2] Wiens et al., *Science Adv.* 8, 34 (2022) [3] Maurice et al., *Space Sci. Rev.* (2021) 217, 47. [4] Wiens et al., *Space Sci. Rev.* (2021) 217, 4. [5] Beck et al., LPSC 2022 #2678 [6] Rapin et al., *Spec. Acta A* (2017) 130, 82. [7] Beck et al., LPSC (2017) #1964 [8] Anderson *Spec. Acta B* 188, 106347(2022) 188, 106347 [9] Forni et al., this meeting [10] Meunier et al., *American Journ. Sci.* (2013) 313, 113. [11] Garzynski this meeting [12] Beyssac et al., this meeting [13] Dehouck et al., this meeting [14] Lopez-Reyes et al., this meeting;

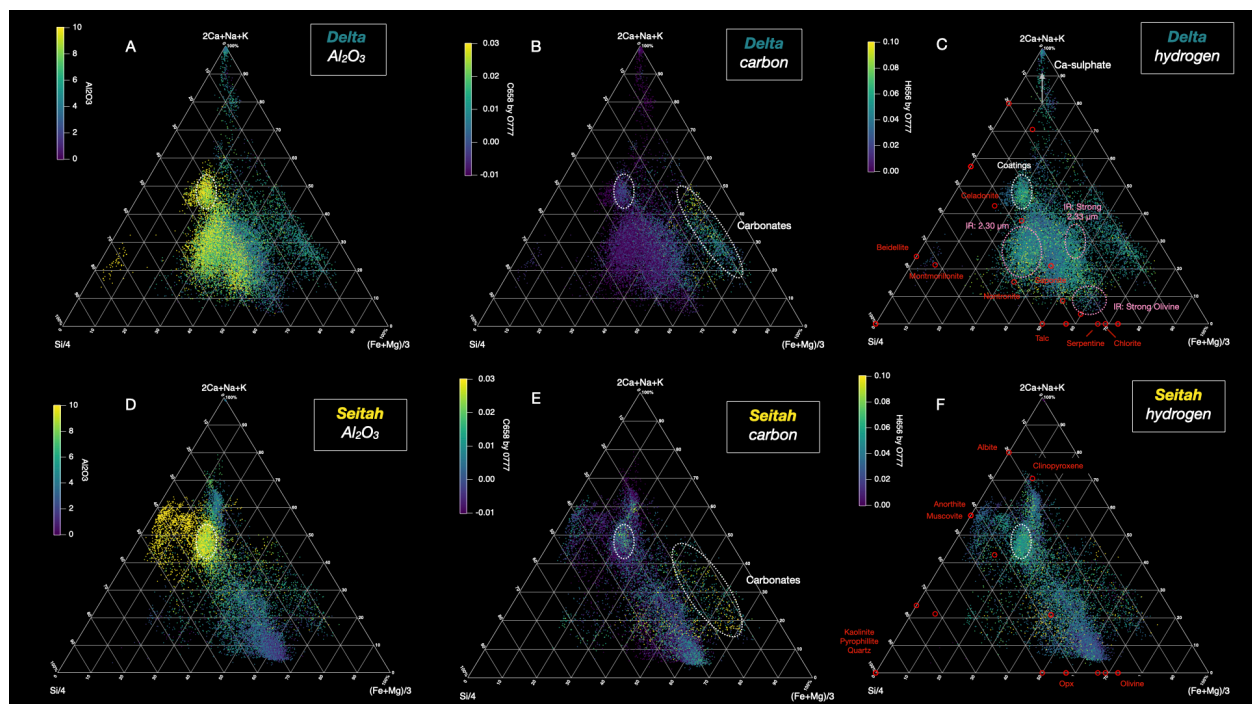


Figure 1: Ternary diagrams for SuperCam LIBS targets. Each point refers to a spectrum of a single-laser shot plasma and is shown here using the Mean Oxide Composition (MOC) derived following Anderson et al. (2022). The diagrams correspond to targets from the delta (A,B,C) as well as target from the Seitah unit (D,E,F). Mineralogical endmembers are also indicated in the diagrams. In all panels, the location of indurated dust coatings on the target is shown as a dashed ellipse (see panel C). The location of targets with a strong 2.33 μm infrared absorption band is also shown in panel as well as targets with strong IR signature of olivine. We also indicate the location of high values of BD2.30-BD2.33, indicating targets where the metal-OH absorption is significant and with a maximum closer to 2.30 than 2.33 μm .